

Mechanical properties of polylactic acid/synthetic rubber blend reinforced with cellulose nanoparticles isolated from kenaf fibres

Mohammad Reza Ketabchi¹ · Chantara Theyy Ratnam² ·
Mohammad Khalid¹ · Rashmi Walvekar³

Received: 23 December 2016 / Revised: 2 May 2017 / Accepted: 10 May 2017
© Springer-Verlag Berlin Heidelberg 2017

Abstract In this work, cellulose nanoparticles (CNP) reinforcement on synthetic rubber (SR)/polylactic acid (PLA) blend was investigated. Initially, SR/PLA blend was prepared by varying SR from 5 to 20 wt%. Later, a fixed amount (3 wt%) of CNP was added and resulting effect on mechanical, thermal, and dynamic properties was studied. The results show the addition of CNP in SR/PLA blend resulted in ~147 and ~196% improvement in tensile strength and storage modulus, respectively. In addition, impact strength of SR/PLA blend was almost doubled after CNP incorporation. An improvement of ~4.5% in the thermal stability of SR/PLA was also observed.

Keywords Cellulose nanoparticles · Natural rubber · Polylactic acid · Biocomposite · Mechanical properties · Thermal properties · Dynamic properties

Introduction

Eco-friendly and cost-effective biocomposite materials have slowly found their position in many sectors including packaging, automotive, household items, medical equipment, and building material industries [1, 2]. The main advantage of biocomposites over petroleum-based composites is their biodegradability and renewability [3]. Development in the use of bioplastic materials in biocomposites is proceeding rapidly; yet, there are several issues such as poor biocompatibility,

✉ Mohammad Khalid
Khalid.Siddiqui@nottingham.edu.my

¹ Department of Chemical and Environmental Engineering, The University of Nottingham Malaysia Campus, Jalan Broga, 43500 Semenyih, Selangor, Malaysia

² Radiation Processing Technology Division, Malaysian Nuclear Agency, Bangi, Malaysia

³ Energy Research Group, School of Engineering, Taylor's University, 47500 Subang Jaya, Selangor, Malaysia

strength, heat resistance, and ease of processing which hinder their applications at large scale. Moreover, the production cost of bioplastics is very high compared to petroleum-based polymers [4]. Among bioplastics, polylactic acid (PLA) is one of the well-known biopolymers mainly due to its high mechanical properties and heat resistance as compared to other bioplastics [5]. Yet, it requires substantial improvements including mechanical properties and thermal stability to be compatible with the conventional plastics.

PLA is one the most favourable thermoplastic aliphatic polyesters, which is fully biodegradable and can be processed similar to polyolefins [6]. It exhibits high stiffness, high tensile strength, and good optical properties that make PLA attractive for many packing and household applications [7]. However, to make PLA also feasible for structural, automotive, and other high performance market applications, new compositions have to be introduced to overcome the low thermal stability, poor toughness, poor impact strength, and poor processability of PLA [8, 9]. Therefore, to improve the mechanical properties of semi-crystalline polymers such as PLA, addition of elastomer is widely reported [10]. Moreover, similarity in the chemical composition of semi-crystalline thermoplastics such as PLA, with elastomers such as synthetic rubber (SR), helps to improve the interfacial interaction in their immiscible blend. Even at low interfacial adhesion, these immiscible blends are widely used, because they produce enough toughening to meet the industry requirements. Similarly, addition of natural elastomers showed to enhance PLA matrix performance [8, 11]. Studies reported a compatible cross-linking between netlike epoxidised NR (ENR) phase and PLA matrix [12]. A sharp transition from brittle to ductile behaviour, and 15 times improvement in impact strength was observed with addition of 40 wt% of ENR to PLA. An improvement in physical and mechanical properties of PLA was reported by adding 10 wt% of SR through melt compounding at 180 °C, 15 min, and 100 rpm [13]. Moreover, addition of 10 wt% of SR toughened PLA composites resulted in higher impact strength and elongation at break values [14]. This is due to the rapid crystallisation that imparts tear growth resistance and high tensile strength properties to SR [15].

Thermal stability of PLA is another drawback which eventually affects its processing and performance in different applications. Low heat distortion temperature (HDT) of PLA limits its applications in biocomposites processed at temperatures exceeding 60 °C [16, 17]. Moreover, due to the degradation of PLA which takes place at about 180 °C, the colour of PLA changes from transparent yellow to light transparent brown which designates thermal degradation [18]. Low HDT could be the main reason that prevents PLA to replace the conventional plastics for higher temperature applications.

To improve the thermal properties and maintain the biodegradability of PLA, reinforcement of lignocellulosic fibres was found beneficial [19]. Processing stability of PLA at 200 °C was confirmed by addition of 5 wt% of cellulose nanoparticles [20]. Thermal stability of composite is directly linked to the crystallinity level of the matrix, and therefore, incorporation of a crystalline fibre such as cellulose was reported favourable. Among wood components, only cellulose is crystalline, while hemicellulose and lignin are non-crystalline. Cellulose has generated lot of interest in both academic and industrial fields due to their

lightweight and worldwide availability. So far, studies are concerned with aspect ratio, geometry, and dispersion of cellulose particles in the matrix, which can notably affect the reinforced biocomposite properties. As a result, research is still active in this area to improve the processing and the performance of such compositions.

Cellulosic fibres are widely available, inexhaustible, and inexpensive material. Bioplastics production is costly; therefore, incorporation of bioplastics with cellulosic fibres can be considered cost-effective. Despite notable improvements and advantages, reinforcement of PLA with cellulosic fibres requires in-depth understanding in several mechanical aspects, especially impact resistance [21]. This is related to the increase in the crystallinity which increases the viscosity of the composites. At high contents, it can notably decrease the composite processability. Increase in the crystalline structure makes the composite fragile that directly affects the impact strength of the composite. It was understood that an optimum amount of SR and cellulose nanoparticles (CNP) could improve impact and tensile strength of PLA, respectively. It was, therefore, found interesting to study if incorporation of an optimum amount of cellulose nanoparticles (CNP) and SR (at the same time) can enhance the thermal and mechanical performance of PLA.

In this study, standard tests were performed to achieve the optimum amount of reinforcement content as well as the best processing condition. The tests include mechanical testing, morphological analysis, thermal gravimetric analysis (TGA), and dynamic mechanical analysis (DMA). Minor drawbacks were observed which were recovered by introducing an SR. SR, a rubbery *cis* 1,4 polyisoprene, is a versatile and adaptable material which has been used successfully in engineering applications [22, 23]. SR has excellent dynamic properties, excellent resistance to fatigue, cut growth and tearing, high resilience, low heat build-up, efficient bonding to reinforcing materials, low cost, and ease of manufacture. However, SR is mainly used as a modifier to improve the bonding between matrix and natural fillers by improving the surface of natural filler [24]. The main advantage of SR over other conventional rubber is its wider range of operating temperature. It has the ability to carry a high load under compression, yet function at high strains and low stiffness compared to metals. In applications where transparency or light colours are required, the application of SR becomes more essential and beneficial as SR has a yellowish-brown hue [25]. This advantage has shifted the attentions of industries and scientists towards the production and use of SR instead of natural rubber. Processing of SR/PLA and CNP/SR/PLA blend was according to the optimised conditions obtained earlier using response surface methodology.

Experimental

Materials

Synthetic Liquid polyisoprene (LIR-30, Molecular weight: 28,000, T_g : -63 °C by Kuraray Co. Ltd., Japan) was used as the plasticiser. Polylactic acid (Ingeo biopolymer, grade 2003 D, melt index 6 g/10 min, density 1.22 g/cm³) was

provided by Nature Works LLC product, USA. CNP was prepared based on our earlier study [26].

Preparation of CNP

CNP was prepared based on our earlier investigation on kenaf fibre through three continues stages of treatment: mercerisation (first stage), bleaching (second stage), and sonication (third stage) [27]. Chemical treatments were done using a vapour line autoclave. The optimal parameters for extraction of CNP were found to be 0.2 g of NaOH/4 g of kenaf fibre at first stage, 5 ml of NaClO₂/4 g of kenaf fibre at the second stage, and 20 min of sonication period during the third stage. Later, compatibility of the extracted CNP with pure PLA was confirmed through our earlier study [28]. Addition of 3 wt% of CNP improved the PLA tensile strength by 25%. Figure 1, presents morphological properties characteristic of the extracted CNP.

Preparation of composite blends

Blends were prepared according to the formulation presented in Table 1 using Brabender PL2000-6 twinscrew compounder at 180 °C, 10 min, and 100 rpm. The optimum composition with highest impact and thermal stability was selected for the preparation of final biocomposite blend (PNR). To prepare PNR, 3 wt% of CNP was gradually added to the stabilised and homogeneous SR/PLA blend.

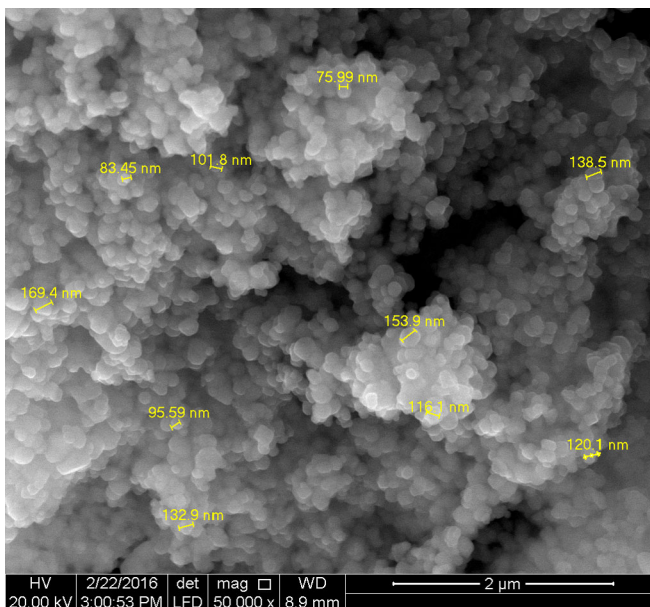


Fig. 1 Scanning electron micrographs of neat CNP

Table 1 Composition and name tags of prepared samples

Sample name	PLA content (wt%)	SR content (wt%)	CNP content (wt%)
PLA	100	–	–
PR1	95	5	–
PR2	90	10	–
PR3	85	15	–
PR4	80	20	–
PNR	87	10	3

Prior to compounding, CNP and PLA granules were dried at 60 °C for 12 h. All compounds were moulded into BS6746 and ASTM D256 standard moulds using a bench top injection moulding machine (RR3400, RAY-RAN Injection Moulding Machine, United Kingdom), at 180 and 90 °C for barrel and mould temperatures, respectively. Holding time for the BS6746 and ASTM D256 samples was 4 and 8 s, respectively. All specimens were conditioned at ambient condition for 48 h before conducting any tests. Pure PLA was used as reference for comparison purpose.

Characterisations

Mechanical properties

Tensile properties The moulded composite samples were tested according to BS6746 standard using tensile tester, TOYOSEIKI Strograph R-1 equipped with a load cell of 1 kN at a crosshead speed of 5 mm min⁻¹. Seven samples for each composition were tested and an average of five repeatable values was taken.

Impact properties All impact samples were cut into rectangular specimens and notched. The Izod impact tests were conducted according to ASTM D256 using CEAST (Model CE UM-636) Impact Pendulum Tester, with a 4 J hammer. Seven specimens were tested and at least five replicate specimens were presented as an average of tested specimens.

Dynamic mechanical analysis (DMA)

Dynamic storage modulus (E'), and mechanical $\tan \delta$ were measured using a dynamic mechanical analyser (Perkin Elmer Diamond DMA Lab System). The scan was made from 30 to 120 °C at 3 °C/min at a frequency of 1 Hz. The samples were cut out to the dimension of 25 × 6 × 2 mm from compression moulded slabs. To establish the experimental reproducibility of DMA data, three identical samples were tested in the same mode and conditions, and the result with reproducible glass transition temperature (T_g) was reported.

Thermal analysis (TGA/DSC)

Thermogravimetric analysis (TGA) and differential scanning calorimetry (DSC) measurements were carried out using Perkin Elmer simultaneous thermal analyser (STA 6000, USA). The TGA was conducted in a nitrogen atmosphere at a heating rate of $10\text{ }^{\circ}\text{C min}^{-1}$ from room temperature to $700\text{ }^{\circ}\text{C}$.

Morphological properties

Fractured tensile and impact samples surface were observed using Field Emission Scanning Electron Microscope (FESEM) (FEI QUANTA 400F) at 20 kV.

Results and discussion

Mechanical properties

Tensile strength and Young's modulus

Mechanical test results including tensile strength and Young's modulus were plotted and presented in Fig. 2a. It is well known that the blend properties are directly influenced by the nature of the matrix and the adhesion between the components [29, 30]. As observed, the addition of 5 wt% SR drastically reduced the tensile strength of the biocomposites blend by $\sim 50\%$. This may be due to different polarities of PLA and SR that makes them immiscible and hence causing defects and voids at the SR/PLA interface resulting in reduced tensile strength. Furthermore, increasing the SR loading the tensile strength dropped steadily. At 20 wt% SR, loading the tensile strength of the biocomposite blend dropped by $\sim 80\%$. Similar drop in the tensile strength was also reported elsewhere, where authors reported composites with high impact properties with notably weak tensile properties. They reported ~ 35 and $\sim 37\%$ reduction in tensile strength of composites (based on addition of 10 wt% of SR in PLA) prepared through melt compounding [13, 14]. Similar trend was observed for tensile modulus also where

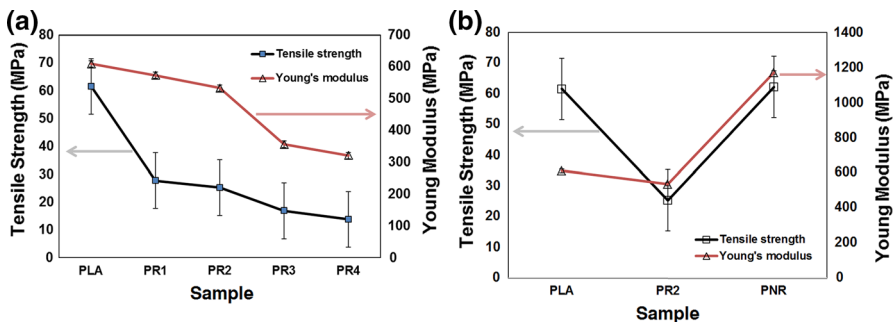


Fig. 2 Tensile strength and modulus: **a** SR/PLA and **b** CNP/SR/PLA

the stiffness of the biocomposite blend decreased with increasing SR loading. In general, the addition of a soft segment of rubber into a hard segment of PLA causes deterioration in the strength and modulus of the blend but improves the elasticity of the blend. Surprisingly, addition of a nucleating agent was also found ineffective to overcome the compatibility issue between PLA and SR [31].

Based on results, addition of up to 10 wt% SR to PLA improved the tensile strength and Young's modulus. Therefore, based on the observations, PR2 composition was selected to blend 3 wt% of CNP for preparation of PNR biocomposites. This was done to recover both the properties of the biocomposite blend. As depicted in Fig. 2b, the addition of CNP in PR2 blend resulted in an exceptional improvement in the tensile strength ($\sim 147\%$) and tensile modulus ($\sim 92\%$) of the biocomposites. The resulting PNR blend values were comparable to the pure PLA value. This drastic improvement in the PNR blend properties was believed to be due to the strong interactions between polymeric groups of PLA and hydroxyl groups of CNP [32, 33]. These active hydroxyl groups acted as a bridge between the two immiscible matrices leading to good compatibilising effects and hence forming continuous phase in the blend.

Impact strength

Figure 3 presents the impact strength of SR/PLA blend and CNP/SR/PLA biocomposite blend. The addition of SR remarkably improved the impact strength of PLA. This may be due to the toughness imparted by rubber phase giving additional movement to the PLA chains and providing an increased flexibility to the blend. The impact strength of PR2 blend was nearly doubled compared to neat PLA samples. As the SR content increased above 10 wt%, the occurrence of voids in PLA matrix becomes more prominent, indicating poor miscibility of the blends. These voids disrupt the continuity of the matrix leading to inefficient transfer of

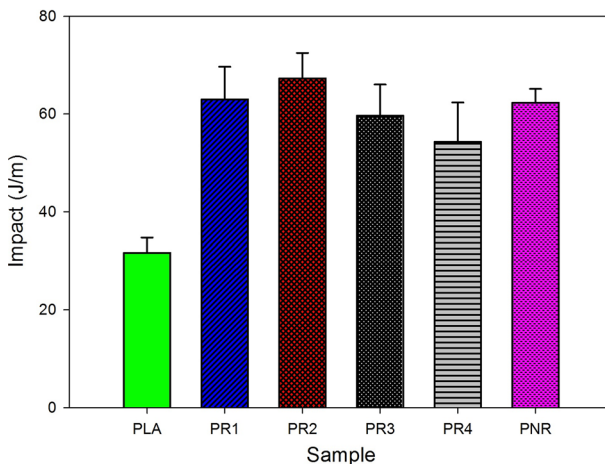


Fig. 3 Impact strength of SR/PLA and CNP/SR/PLA biocomposites

stress within the matrix. Moreover, reduction in area, due to a crack or void, results in a localised increase in stress. A material can fail, via a propagating crack, when a concentrated stress exceeds the material's theoretical cohesive strength. This is also evident from the results where 20 wt% SR loading shows the lower impact properties compared to 10 wt% SR loading. However, even at 20 wt% SR loading, it should be noted that the impact strength was reasonably higher (36%) compared to Pure PLA.

The addition of 3 wt% CNP to the blend with SR and PLA slightly reduced its impact strength by 10% (PNR compared to PR2), indicating the change in the properties of blend from ductile to brittle. This is also evident from the FESEM analysis (Fig. 11c) showing a wavy fractured pattern which corresponds to brittle fracture. This transition in the property of the blend is attributed to the improved interfacial bonding between two immiscible matrices due to the addition of CNP. During the impact, the brittle samples work hardens without undergoing plastic deformation at the notch, which significantly reduces the energy absorbing capacity of the material leading to brittle fracture of the sample. However, the presence of SR as a toughener helped in retaining the impact strength of the PNR biocomposite blend. The other reason for the decline in the PNR blend impact property could be due to the agglomeration of CNP which might act as stress concentration point, resulting in a localised increase in the stress, leading to early failure of the samples. However, it is clear that the presence of SR and CNP was essential to maintain tensile properties of PLA while improving its impact resistant properties.

Dynamical properties

Storage modulus (E')

To study the viscoelastic behaviour of biocomposites, storage modulus (E') was estimated. Higher E' values indicated the rigidity of biocomposites. Samples glass transition (T_g) temperature was obtained based on their damping factor (α). E' value decreased through all samples with increasing temperature (Fig. 4a, b). This was

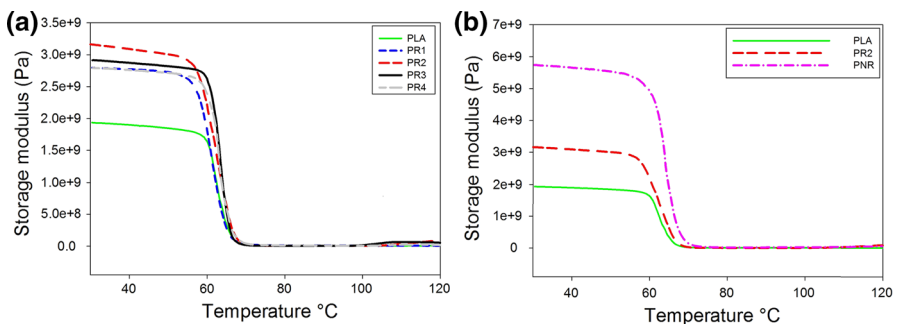


Fig. 4 Viscoelastic behaviour (storage modulus): **a** SR/PLA and **b** CNP/SR/PLA

linked to the increase in viscosity and flexibility of polymer chains which reduced the rigid interface between CNP and PR2 matrix [34, 35].

As the temperature increased to 120 °C, PR2, PR3, PR4, and PNR compositions showed much higher storage modulus values than that of PLA. This was due to the stress transfer from PLA to both SR and CNP while as observed, CNP showed greater capabilities in this case. In addition, reinforcement of rigid nano filler like CNP increases the biocomposite stiffness and thermal stability. This was observed both in dynamical and thermal analysis as PNR samples revealed superior properties. This was linked to the preparation process of CNP which notably reduced its moisture absorbing capacity. Hydrophobic fibres show better wetting ability as compared to hydrophilic fibres and result in stronger bonding with the rubber matrix; moisture content acts as a barrier and prevents the wetting process. The improvement in storage modulus for PNR samples was also linked to the high surface area of CNP (Fig. 1). Higher surface area of nanoparticles led to a better interaction within the matrix and resulted higher storage modulus values than PR samples. To further study the incorporation influence of CNP with PR2 matrix, the relative normalised storage modulus (E^*) was calculated using Eq. 1 and the results were presented in Fig. 5:

$$E^* = E'_C / E'_m \tag{1}$$

where E'_C and E'_m were storage modulus of biocomposites and PLA matrix, respectively, with selected temperatures at different nanofiller loadings. The values were more pronounced at higher temperatures (above T_g). As expected, the results revealed an increase in storage modulus value for all PR samples with increase in SR content, while this improvement was best presented in PR2 samples. Therefore, PR2 was approved to be the suitable composition to host CNP for preparation of PNR samples. PNR samples showed notably higher storage modulus values as compared to all samples including PLA. This was due to the improvement in

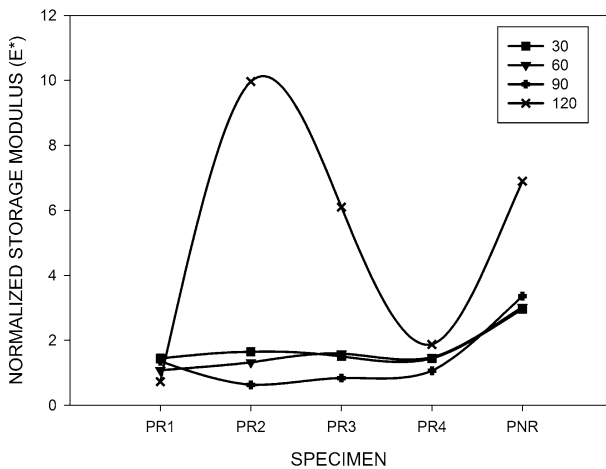


Fig. 5 Normalised storage modulus of SR/PLA and CNP/SR/PLA biocomposites

Table 2 Variations of biocomposites modulus retention

Specimen	<i>C</i>	Modulus retention %		
		E'_{60}/E'_{30}	E'_{90}/E'_{30}	E'_{120}/E'_{30}
PLA	–	83.43	0.32	0.46
PR1	1.98	62.44	0.30	0.23
PR2	0.16	66.91	0.12	2.82
PR3	0.24	88.24	0.17	1.88
PR4	0.76	85.49	0.23	0.60
PNR	0.42	85.27	0.36	1.08

thermal stability of the composition followed by the addition of CNP. However, at 120 °C, it should be noted that PR2 presented a slightly higher storage modulus value than PNR which was linked to the minor degradation of CNP at ~ 120 °C.

Through similar studies, samples showed higher E' values at their rubbery state as compared to glassy state [36]. Above T_g , the variance in E' values was easily distinguished due to the matrix shift from glassy state to rubbery state. The variation of biocomposites modulus retention was presented in Table 1. The influence of CNP and SR on the modulus of the PLA matrix was determined and validated by coefficient “*C*” using Eq. 2; where E'_G and E'_R were storage modulus values in glassy and rubbery regions, respectively. The obtained E' values at 30 and 120 °C were arbitrarily selected (below and above T_g) as E'_G and E'_R , respectively. Lower “*C*” values were preferred as they were presenting higher efficiency of reinforcing PLA matrix with SR and CNP, respectively (Table 2):

$$C = ((E'_G/E'_R))_{\text{biocomposites}} / ((E'_G/E'_R))_{\text{PLA}} \quad (2)$$

When comparing the PR samples, the addition of SR to PLA matrix more than 10 wt% was found less beneficial to obtain a favourable “*C*” value. This was linked to the increase in samples elasticity at higher SR contents [37]. Incorporation of CNP into PR2 retained the *C* value at low level and slightly improved the modulus retention values.

Tangent delta (*tan δ*)

The $\tan \delta$ curves as a function of temperature were determined and studied using Eq. 3. The $\tan \delta$ curves were presented in Fig. 6:

$$\tan \delta = E''/E' \quad (3)$$

Samples T_g was estimated based on the main peak of $\tan \delta$ curve [38]. Samples had relatively close T_g values. It was observed that PLA, PR1, PR2, PR3, PR4, and PNR samples have a T_g value of 68.99, 68.31, 69.65, 69.08, 69.61, and 70.80 °C, respectively. PLA and PR blends showed relatively similar thermograms, showing that SR had a minor influence on cold crystallisation of PLA phase. Similar results were reported by Chuanhui et al., where like compositions were prepared [39]. High

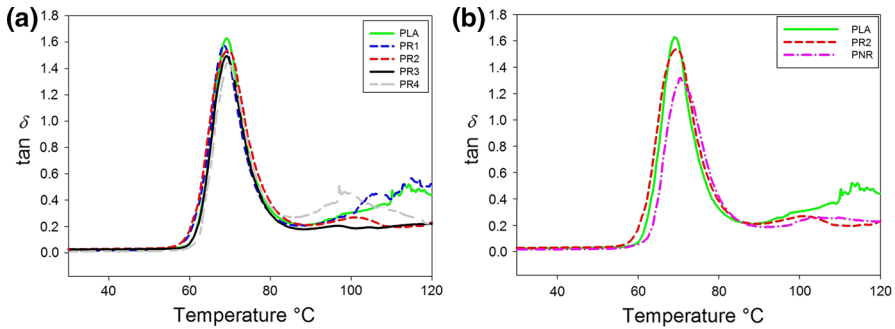


Fig. 6 Viscoelastic behaviour ($\tan \delta$); **a** SR/PLA and **b** CNP/SR/PLA

immiscibility encourages coalescence of the dispersed phase as phase separation is preferred in such blends. Increase in the SR content (PR1–PR4) increased the immiscibility between PLA and SR; therefore, the SR dispersed particles clustered in their phase causing the coalescence. As comparing PR2 with PNR, the slight shift in T_g value from 69.65 to 70.80 °C was linked to the reduction in rubber chain mobility [13, 40]. This was due to the incorporation of high-energy surface of CNP as it strongly interacted with PLA matrix and improved its abrasion and tear resistance and shifted its affinity toward elastomeric phase [41, 42]. Apparently thermal history and molecular mobility play more important roles in the determination of relaxation processes and glass transition than interactions.

Through similar studies, scientists linked the height of the $\tan \delta$ to the motion of free main segments of molecular chains [43]. The addition of SR and later CNP notably reduced this motion and decreased the height, respectively (Fig. 6a, b). In addition, in terms of damping, the increase in SR content was found beneficial as it slightly decreased the PLA $\tan \delta$ value. This value notably decreased following the introduction of CNP to PR2/PLA matrix. This was found to be due to the nanofiller toughening effect as well as increase in biocomposites elastic response [44, 45]. Also following the preparation method, it could be due to the sheared surface of nano filler particles which allow a better stress transfer [34]. Samples elasticity behaviour can be directly influenced by the damping (molecular mobility) in the stress transition region [46]. In this study, this negative influence was reduced by incorporation of CNP as the stress was transferred from matrix to the nano fillers. Similar observations were obtained as scientists reinforced polyurethane matrix with CNP [47]. This improvement was related to the strong physical H bonding and covalent linkages between the matrix and the nanofiller.

Thermal properties

TGA

Throughout all compositions, the addition of SR was found favourable. PR2 showed to have the highest thermal stability as compared to PR1, PR3, and PR4 (Fig. 7). In conjunction with morphological, mechanical, and dynamical results, thermal

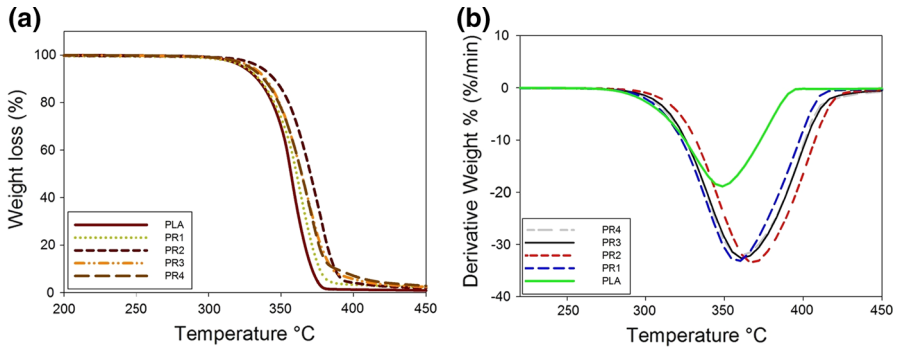


Fig. 7 SR/PLA blend TGA and DTG curves

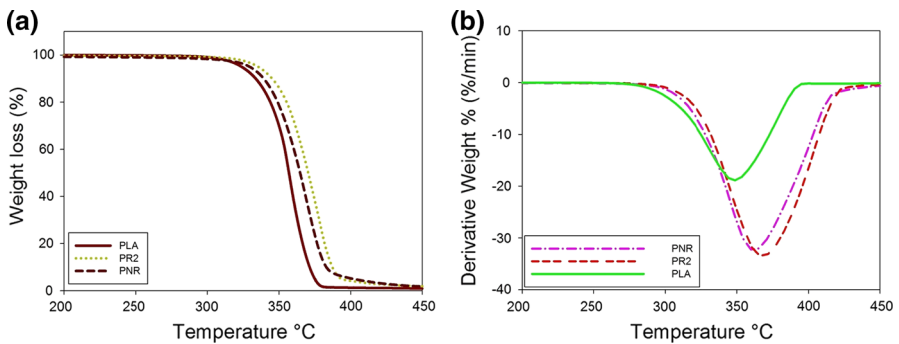


Fig. 8 CNP/SR/PLA blend TGA and DTG curves

analysis agreed on selection of PR2 as the optimum composition. Later, the addition of CNP to PR2 composition enhanced the thermal stability of PLA by $\sim 20^\circ\text{C}$ (Fig. 8). CNP has a hydrogen-bonded structure that leads to a low thermal conductivity during thermal degradation [48]. The resistance in thermal conductivity delayed the weight loss of the reinforced biocomposite, and therefore, the overall thermal stability of PNR was enhanced. In addition, the thermal improvement was linked to the preparation technique of CNP which was designed to improve the nanoparticles thermal stability by removing lignin and hemicellulose from kenaf fibre. Meanwhile, PNR showed lower thermal stability as compared to PR2 which was linked to the degradation of CNP at high temperatures (above 300°C).

Thermal analysis is important to investigate thermal decomposition of biocomposites. The weight loss of biocomposites due to formation of volatile materials after degradation as a function of temperature was summarised in Table 3. For each sample, three stages of weight loss were selected [after 10% (T_{10}), 50% (T_{50}), and 90% (T_{90})]. Overall, it was observed that T_{10} , T_{50} , and T_{90} of PLA increased with increase in both SR and CNP contents. As comparing the results at T_{90} , 10 wt% of SR (PR2) increased the thermal stability of PLA by 4%, while the combination of

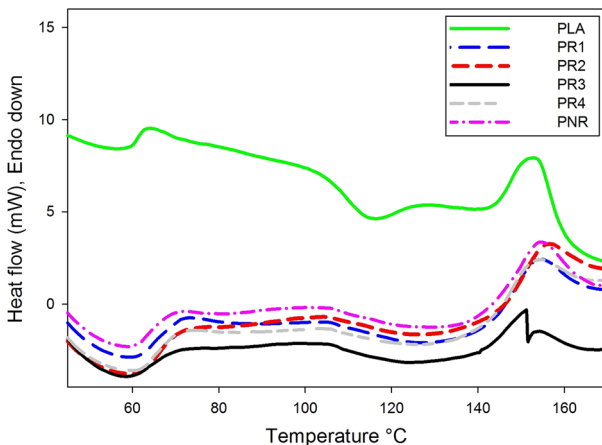
Table 3 TGA results for PLA, PR, and PNR biocomposites

Sample name	T ₁₀	T ₅₀	T ₉₀
PLA	333.71	356.64	371.24
PR1	334.68	360.42	376.6
PR2	345.15	369.93	387.09
PR3	339.37	363.79	385.24
PR4	338.03	363.83	387.73
PNR	339.32	364.34	382.87

10 wt% of SR and 3 wt% of CNP (PNR) increased this value by 3%. Hence, in this case, the effect of SR on thermal stability of PLA was more sensible as compared to CNP. This improvement was observed up to addition of 10 wt% of SR and at higher concentrations declining effect on thermal stability of PLA was detected.

DSC

In addition to TGA, DSC analysis was carried out to further analyse the structure of PLA with addition of SR and CNP. The results of this analysis were presented in Fig. 9. T_g , (determined at the peak of exothermic area) and melting temperature (T_m) (determined at the peak of endothermic melting area) were observed. It was earlier observed that the T_g of all PR and PNR blends was located at nearly same temperature ($\sim 70^\circ\text{C}$). This indicated that the addition of SR and CNP did not have a noticeable effect on the glass transition behaviour of PLA. Studies reported similar behaviour (minor change in T_g value with addition of SR) and average T_g values at ~ 58 , ~ 63 , $\sim 62^\circ\text{C}$ were reported, respectively [49–51]. The results in this study were approximately 10°C higher as compared to the mentioned studies, which was linked to the optimised interaction between SR and PLA matrix which increased its stability, and therefore, higher glass transition value was obtained. Above T_g , PLA

**Fig. 9** DSC curves of PLA and PLA-based blends

performed an aging peak in the range from 70 to 90 °C which was related to the aging of amorphous polymer [50]. This observation became less sensible for other samples (especially for PNR), as crystalline structures (SR and CNP) were introduced with the addition of SR. The double peak melting point of PR3 (at 151.25 and 153.97 °C) was linked to two stages of melting. This mainly happens for biocomposites with non-homogeneous structure; more perfect crystalline structures melt at higher temperatures and, therefore, result in two peaks [52]. PLA melting point (T_m) was observed at 152.43 °C, while with a slight increase, PR2 and PNR melted at 157.18 and 154.49 °C. The slight delay in melting point of PLA was similarly linked to the increase in crystalline structure of biocomposite with addition of SR and CNP as the viscosity and flexibility of polymer chains were increased.

Morphological properties

Two individual phases in the SR/PLA blends were detectible (Fig. 10). During both tensile and impact test, many SR particles were pulled out from the PLA matrix and voids were created (Fig. 10a, b). As comparing Fig. 10a with c, it was observed that the biocomposite morphology became more complex and flocculated with increase in SR content. This showed the adequacy and compatibility of 10 wt% of SR blended with PLA. This was related to the increase in the interaction between the two components (SR and PLA). Samples PR3 and PR4 presented notable air pockets, which were linked to the air bubbles that were introduced during the preparation process (highlighted in Fig. 10e–h). In addition to thermal and mechanical observations, the morphological studies agreed on the inefficiency of PR3 and PR4 compositions for a desirable performance. The voids had their negative influence on mechanical properties and notably decreased the tensile strength of samples (Fig. 2).

The voids did not only affect the tensile performance, but also the impact resistance of samples. The effectiveness of SR is controlled by many factors such as type and blend ratio of rubber, size and shape of the rubber phase, interaction between rubber particles and matrix, compounding process, processing temperature, etc. At concentrations higher than 10 wt% of SR, the voids were created and prevented SR to play its role as a plasticiser and declining results on impact strength were detected (Fig. 3). It was understood that the improvement in the impact strength of PR2 was directly linked to the optimum interfacial adhesion between SR and PLA.

A detailed discussion about CNP thermal, structural, and morphological properties was presented in our earlier study [27]. One of the main drawbacks of CNP is the aggregation, which could result in an inhomogeneous stress transfer from matrix to nanoparticles. The presence of SR and selection of compounding process instead of solvent casting were the two solutions found to this issue. As observed in Fig. 1, CNP appeared in aggregated nanospherical shapes prior to reinforcement, while the same nanoparticles were less aggregated and evenly dispersed after the reinforcement process (Fig. 11b). It was understood that SR made nanoparticles movement easier through the matrix and the shearing force through compounding enforced the nanoparticles to form homogeneously.

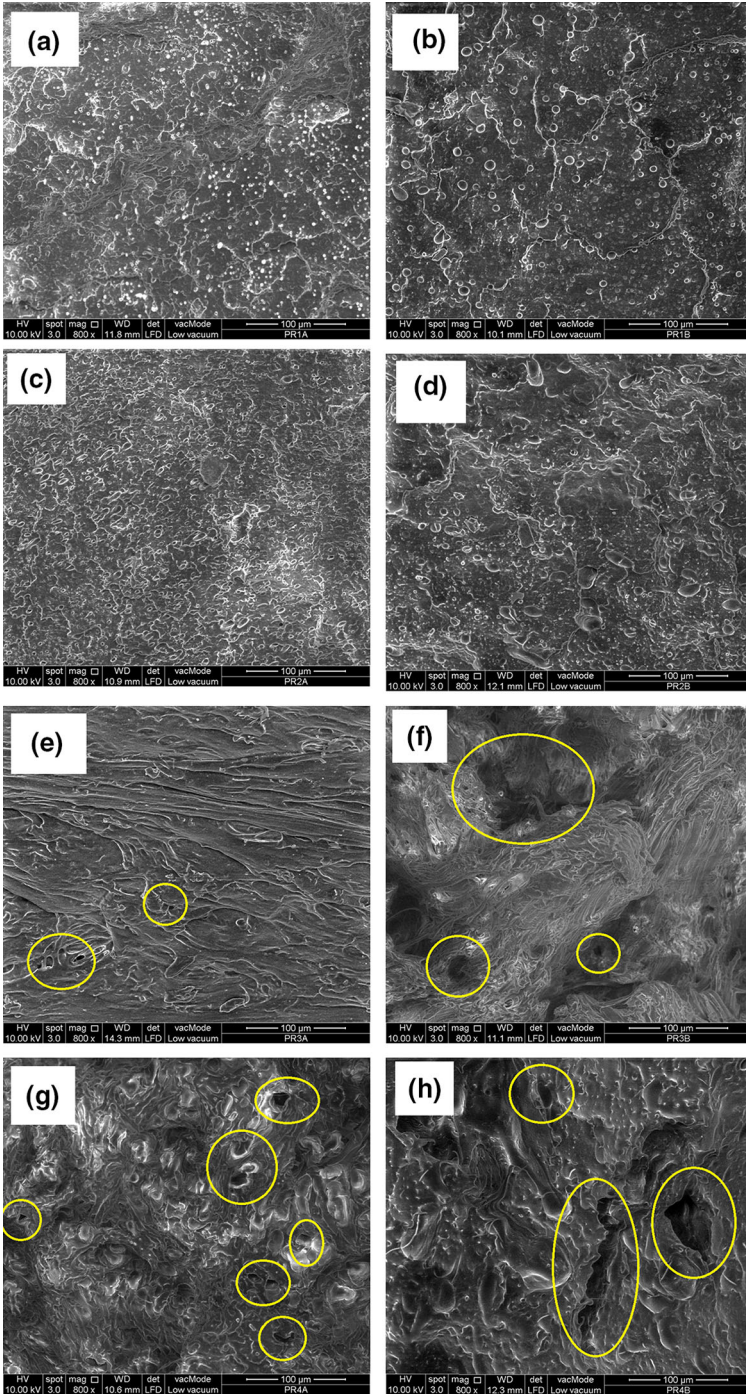


Fig. 10 Biocomposites scanning electron micrographs; tensile fracture surface of **a** R1, **c** PR2, **e** PR3, and **g** PR4; Izod impact fracture surface of **b** PR1, **d** PR2, **f** PR3, and **h** PR4

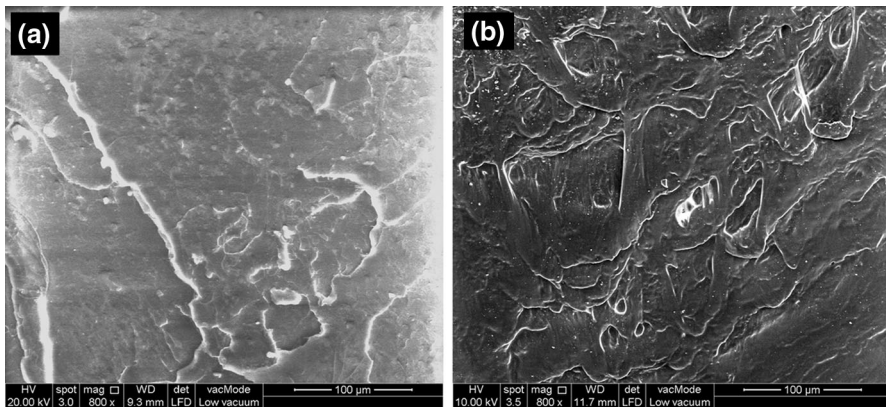


Fig. 11 Scanning electron micrographs of **a** PLA and **b** PNR

Figure 11a shows the failure of PLA matrix due to brittle fracture as indicated by the appearance of wavy lines and smooth fracture surface. The addition of SR as a plasticiser notably reduced the brittle structure of PLA and increased the ductility of the composite blend. However, at higher concentrations of SR, an uneven dispersion of SR in the PLA matrix was observed, leaving some voids in the PLA matrix. The very clear interface between the PLA matrix and SR particles can be attributed to poor interfacial compatibility between the two phases at higher SR content that later notably affected tensile strength properties of composite blend.

Conclusions

In this study, SR/PLA biocomposites were reinforced with 3 wt% of CNP through melt compounding technique. It was observed that PLA with 10 wt% of SR was found to be the optimum composition to host 3 wt% of CNP. Incorporation of 3 wt% CNP in SR/PLA blend resulted in ~147, ~196, and ~200% improvement in tensile strength, storage modulus, and impact strength, respectively. The addition of CNP also enhanced the viscoelastic behaviour of PR2 blend and also reducing the damping effect. Moreover, the presence of SR resulted in a homogeneous dispersion of CNP in the blend. The addition of CNP together with SR was found essential to retain both the tensile properties and impact resistant properties of SR/PLA blend.

References

1. AL-Oqla FM, Allothman OY, Jawaid M, Sapuan S, Es-Saheb M (2014) Processing and properties of date palm fibers and its composites. In: Hakeem KR, Jawaid M, Rashid U (eds) Biomass Bioenergy, vol 1. Springer, Cham, Switzerland, pp 1–25. doi:10.1007/978-3-319-07641-6_1
2. Râpă M, Miteluț AC, Tănase EE, Grosu E, Popescu P, Popa ME et al (2016) Influence of chitosan on mechanical, thermal, barrier and antimicrobial properties of PLA-biocomposites for food packaging. Compos B Eng 102:112–121

3. Veccharelli KM, Tong VK, Young JL, Yang J, Gianneschi NC (2016) Dual responsive polymeric nanoparticles prepared by direct functionalization of polylactic acid-based polymers via graft-from ring opening metathesis polymerization. *Chem Commun* 52(3):567–570
4. Xu H, Yang Y (2012) *Bioplastics from waste materials and low-value byproducts. Degradable polymers and materials: principles and practice*, 2nd edn. ACS Publications, United States, pp 113–140. doi:10.1021/bk-2012-1114.ch008
5. Frone AN, Berlioz S, Chailan J-F, Panaitescu DM (2013) Morphology and thermal properties of PLA–cellulose nanofibers composites. *Carbohydr Polym* 91(1):377–384
6. Lim L-T, Auras R, Rubino M (2008) Processing technologies for poly (lactic acid). *Prog Polym Sci* 33(8):820–852
7. Marra A, Silvestre C, Duraccio D, Cimmino S (2016) Polylactic acid/zinc oxide biocomposite films for food packaging application. *Int J Biol Macromol* 88:254–262
8. Bitinis N, Verdejo R, Cassagnau P, Lopez-Manchado M (2011) Structure and properties of polylactide/natural rubber blends. *Mater Chem Phys* 129(3):823–831
9. Hashima K, Nishitsuji S, Inoue T (2010) Structure-properties of super-tough PLA alloy with excellent heat resistance. *Polymer* 51(17):3934–3939
10. Ock HG, Kim DH, Ahn KH, Lee SJ, Maia JM (2016) Effect of organoclay as a compatibilizer in poly (lactic acid) and natural rubber blends. *Eur Polymer J* 76:216–227
11. Wu N, Zhang H, Fu G (2016) Super-tough poly (lactide) thermoplastic vulcanizates based on modified natural rubber. *ACS Sustain Chem Eng* 5(1):78–84
12. Wang Y, Chen K, Xu C, Chen Y (2015) Supertoughened biobased poly (lactic acid)–epoxidized natural rubber thermoplastic vulcanizates: fabrication, co-continuous phase structure, interfacial in situ compatibilization, and toughening mechanism. *J Phys Chem B* 119(36):12138–12146
13. Bitinis N, Verdejo R, Maya EM, Espuche E, Cassagnau P, Lopez-Manchado MA (2012) Physicochemical properties of organoclay filled polylactic acid/natural rubber blend bionanocomposites. *Compos Sci Technol* 72(2):305–313
14. Jaratrotkamjorn R, Khaokong C, Tanrattanakul V (2012) Toughness enhancement of poly (lactic acid) by melt blending with natural rubber. *J Appl Polym Sci* 124(6):5027–5036
15. Jawaid M, Khalil HA, Hassan A, Dungani R, Hadiyane A (2013) Effect of jute fibre loading on tensile and dynamic mechanical properties of oil palm epoxy composites. *Compos B Eng* 45(1):619–624
16. Spinella S, Re GL, Liu B, Dorgan J, Habibi Y, Leclere P et al (2015) Polylactide/cellulose nanocrystal nanocomposites: efficient routes for nanofiber modification and effects of nanofiber chemistry on PLA reinforcement. *Polymer* 65:9–17
17. Braun B, Dorgan JR (2008) Single-step method for the isolation and surface functionalization of cellulosic nanowhiskers. *Biomacromol* 10(2):334–341
18. Oksman K, Mathew AP, Bondeson D, Kvien I (2006) Manufacturing process of cellulose whiskers/polylactic acid nanocomposites. *Compos Sci Technol* 66(15):2776–2784
19. Jang JY, Jeong TK, Oh HJ, Youn JR, Song YS (2012) Thermal stability and flammability of coconut fiber reinforced poly (lactic acid) composites. *Compos B Eng* 43(5):2434–2438
20. Petersson L, Kvien I, Oksman K (2007) Structure and thermal properties of poly(lactic acid)/cellulose whiskers nanocomposite materials. *Compos Sci Technol* 67(11–12):2535–2544
21. Porras A, Maranon A (2012) Development and characterization of a laminate composite material from polylactic acid (PLA) and woven bamboo fabric. *Compos B Eng* 43(7):2782–2788
22. Waser H (1974) Elastomer blends and tire sidewalls prepared therefrom. Google Patents
23. Dinsmore RP (1929) Synthetic rubber and method of making it. Google Patents
24. Suttivutnarubet C, Jaturapiree A, Chaichana E, Prasertthdam P, Jongsomjit B (2016) Synthesis of polyethylene/coir dust hybrid filler via in situ polymerization with zirconocene/MAO catalyst for use in natural rubber biocomposites. *Iran Polym J* 25(10):841–848
25. Shimizu A, Kusano M, Takami T (1977) Rubber compositions and methods for production thereof stabilized. Google Patents
26. Mohammad Reza K, Mohammad K, Chantara TR, Rashmi W, Md Enamul H (2016) Sonosynthesis of cellulose nanoparticles (CNP) from Kenaf fibre: effects of process parameters. *Fibers Polym* 17(9):1352–1358
27. Ketabchi MR, Khalid M, Ratnam CT, Manickam S, Walvekar R, Hoque ME (2016) Sonosynthesis of cellulose nanoparticles (CNP) from kenaf fiber: effects of processing parameters. *Fibers Polym* 17(9):1352–1358

28. Ketabchi MR, Khalid M, Ratnam CT, Walvekar R (2016) Mechanical and thermal properties of polylactic acid composites reinforced with cellulose nanoparticles extracted from kenaf fibre. *Mater Res Express* 3(12):125301
29. Wan Y, Luo H, He F, Liang H, Huang Y, Li X (2009) Mechanical, moisture absorption, and biodegradation behaviours of bacterial cellulose fibre-reinforced starch biocomposites. *Compos Sci Technol* 69(7):1212–1217
30. Granda L, Espinach F, Tarrés Q, Méndez J, Delgado-Aguilar M, Mutjé P (2016) Towards a good interphase between bleached kraft softwood fibers and poly (lactic) acid. *Compos Part B Eng* 99:514–520. doi:[10.1016/j.compositesb.2016.05.008](https://doi.org/10.1016/j.compositesb.2016.05.008)
31. Suksut B, Deeprasertkul C (2011) Effect of nucleating agents on physical properties of poly(lactic acid) and its blend with natural rubber. *J Polym Environ* 19(1):288–296
32. Li X, Tabil LG, Panigrahi S (2007) Chemical treatments of natural fiber for use in natural fiber-reinforced composites: a review. *J Polym Environ* 15(1):25–33
33. Lee S-Y, Mohan DJ, Kang I-A, Doh G-H, Lee S, Han SO (2009) Nanocellulose reinforced PVA composite films: effects of acid treatment and filler loading. *Fibers Polym* 10(1):77–82
34. Khalid M, Ratnam CT, Abdullah LC, Walvekar R, Ching YC, Ketabchi MR (2016) Mechanical and physical performance of cowdung-based polypropylene biocomposites. *Polym Compos*. doi:[10.1002/pc.23928](https://doi.org/10.1002/pc.23928)
35. Zaaba NF, Ismail H, Jaafar M (2015) A study of the degradation of compatibilized and uncompatibilized peanut shell powder/recycled polypropylene composites due to natural weathering. *J Vinyl Addit Technol*. doi:[10.1002/vnl.21504](https://doi.org/10.1002/vnl.21504)
36. Grigoriadi K, Giannakas A, Ladavos AK, Barkoula N-M (2015) Interplay between processing and performance in chitosan-based clay nanocomposite films. *Polym Bull* 72(5):1145–1161
37. Nair KG, Dufresne A (2003) Crab shell chitin whisker reinforced natural rubber nanocomposites. 2. Mechanical behavior. *Biomacromolecules-Washington* 4(3):666–674
38. Gong X, Liu J, Baskaran S, Voise RD, Young JS (2000) Surfactant-assisted processing of carbon nanotube/polymer composites. *Chem Mater* 12(4):1049–1052
39. Xu C, Yuan D, Fu L, Chen Y (2014) Physical blend of PLA/NR with co-continuous phase structure: preparation, rheology property, mechanical properties and morphology. *Polym Test* 37:94–101
40. Gregorova A, Sedlarik V, Pastorek M, Jachandra H, Stelzer F (2011) Effect of compatibilizing agent on the properties of highly crystalline composites based on poly(lactic acid) and wood flour and/or mica. *J Polym Environ* 19(2):372–381
41. Pei A, Zhou Q, Berglund LA (2010) Functionalized cellulose nanocrystals as biobased nucleation agents in poly (l-lactide)(PLLA)—crystallization and mechanical property effects. *Compos Sci Technol* 70(5):815–821
42. Bokobza L (2004) The reinforcement of elastomeric networks by fillers. *Macromol Mater Eng* 289(7):607–621
43. Kang H, Qiao B, Wang R, Wang Z, Zhang L, Ma J et al (2013) Employing a novel bioelastomer to toughen polylactide. *Polymer* 54(9):2450–2458
44. Quresimin M, Schulte K, Zappalorto M, Chandrasekaran S (2016) Toughening mechanisms in polymer nanocomposites: from experiments to modelling. *Compos Sci Technol* 123:187–204
45. Sun Q, Mekonnen T, Misra M, Mohanty AK (2016) Novel biodegradable cast film from carbon dioxide based copolymer and poly(lactic acid). *J Polym Environ* 24(1):23–36
46. Ropers S, Kardos M, Osswald TA (2016) A thermo-viscoelastic approach for the characterization and modeling of the bending behavior of thermoplastic composites. *Compos Part A Appl Sci Manuf* 90:22–32. doi:[10.1016/j.compositesa.2016.06.016](https://doi.org/10.1016/j.compositesa.2016.06.016)
47. Aranguren MI, Marcovich NE, Salgueiro W, Somoza A (2013) Effect of the nano-cellulose content on the properties of reinforced polyurethanes. A study using mechanical tests and positron annihilation spectroscopy. *Polym Test* 32(1):115–122
48. Lee C-K, Cho MS, Kim IH, Lee Y, Do Nam J (2010) Preparation and physical properties of the biocomposite, cellulose diacetate/kenaf fiber sized with poly (vinyl alcohol). *Macromol Res* 18(6):566–570
49. Jawaid M, Abdul Khalil HPS, Alattas OS (2012) Woven hybrid biocomposites: dynamic mechanical and thermal properties. *Compos A Appl Sci Manuf* 43(2):288–293
50. Zhang C, Wang W, Huang Y, Pan Y, Jiang L, Dan Y et al (2013) Thermal, mechanical and rheological properties of polylactide toughened by expoxidized natural rubber. *Mater Des* 45:198–205

51. Cao X, Mohamed A, Gordon S, Willett J, Sessa D (2003) DSC study of biodegradable poly (lactic acid) and poly (hydroxy ester ether) blends. *Thermochim Acta* 406(1):115–127
52. Sarasua J-R, Prud'Homme RE, Wisniewski M, Le Borgne A, Spassky N (1998) Crystallization and melting behavior of polylactides. *Macromolecules* 31(12):3895–3905